The *Drosophila* Class B Scavenger Receptor NinaD-I Is a Cell Surface Receptor Mediating Carotenoid Transport for Visual Chromophore Synthesis†

Olaf Voolstra, Cornelia Kiefer, Martin Hoehne,‡ Ralf Welsch,§ Klaus Vogt, and Johannes von Lintig*

Institute of Biology I, University of Freiburg, Hauptstrasse 1, D-79104 Freiburg im Breisgau, Germany

Received April 11, 2006; Revised Manuscript Received September 8, 2006

ABSTRACT: The blind *Drosophila* mutant *ninaD* lacks the visual chromophore. Genetic evidence that the molecular basis is a defect in carotenoid uptake which causes vitamin A deficiency exists. The *ninaD* gene encodes a scavenger receptor that is significantly homologous in sequence with the mammalian scavenger receptors SR-BI (scavenger receptor class B type I) and CD36 (cluster determinant 36), yet NinaD has not been characterized in functional detail. Therefore, we established a *Drosophila* S2 cell culture system for biochemically characterizing the *ninaD* gene products. We show that the two splice variant isoforms encoded by *ninaD* exhibit different subcellular localizations. NinaD-I, the long protein variant, is localized at the plasma membrane, whereas the short variant, NinaD-II, is localized at intracellular membranes. Only NinaD-I could mediate the cellular uptake of carotenoids from micelles in this cell culture system. Carotenoid uptake was concentration-dependent and saturable. By in vivo analyses of different mutant and transgenic fly strains, we provide evidence of an essential role of NinaD-I in the absorption of dietary carotenoids to support visual chromophore synthesis. Moreover, our analyses suggest a role of NinaD-I in tocopherol metabolism. Even though *Drosophila* is a sterol auxotroph, we found no evidence of a contribution of NinaD-I to the uptake of these compounds. Together, our study establishes an evolutionarily conserved connection between class B scavenger receptors and the numerous functions of fat soluble vitamins in animal physiology.

Dietary lipids comprise a class of structurally diverse compounds that includes fatty acids, acylglycerols, lysophospholipids, sterols, and fat soluble vitamins. Besides being important for energy metabolism, these lipids or metabolites thereof serve as signaling molecules (*1*) and structural components of membranes. To become biologically active, dietary lipids have to be absorbed in the gut and transported to target tissues for further metabolism or storage. Strong evidence has been provided that the absorption of dietary lipids in the gut is a regulated protein-mediated process involving, e.g., ABC transporters (*2*), scavenger receptors (*3*), and the Niemann Pick C1 Like 1 (NPC1L1) protein (*4*). However, the exact role of these transporters in lipid metabolism is still a matter of debate.

Scavenger receptor class B type I (SR-BI) has been suggested to be a key component in lipid transport processes. In mammals, this 82 kDa transmembrane protein is predominantly expressed in liver and steroidogenic tissues (*5*, *6*). SR-BI binds circulating high-density lipoproteins (HDLs) via their apolipoprotein components (*7*), facilitating transfer of cholesteryl ester from HDL into target cells (*8*). SR-BI can also mediate the bidirectional flux of unesterified cholesterol between serum lipoproteins and cells (*9*, *10*). Thus, SR-BI contributes to supplying target tissues with cholesteryl esters but also to eliminating excess cholesterol from peripheral tissues and transporting it to the liver, a process termed reverse cholesterol transport (*11*). Additionally, SR-BI contributes to the selective uptake of HDL-associated vitamin E, as shown in porcine brain (*12*) and rat pneumocytes (*13*).

Recent studies have provided evidence for an additional role of SR-BI in enterocytes of the gut epithelium, where this receptor may facilitate the absorption of cholesterol from mixed micelles (*3*). There is evidence that SR-BI in the gut also acts in the uptake of other dietary isoprenoid compounds such as tocopherols (*14*) and carotenoids (*15*, *16*). Animals retain considerable amounts of these compounds; e.g., the central part of the primate retina, the *macula lutea*, owes its yellow color to high levels of the carotenoids lutein and zeaxanthin (*17*, *18*). This specific accumulation of carotenoids supports the idea of specific uptake and retention mechanisms for these compounds within respective tissues and reflects their physiological importance. Additionally, certain carotenoids are precursors for retinoids (vitamin A and its derivatives). To yield retinoids, carotenoids have to be oxidatively cleaved by β-carotene-15,15′-monooxygenase (Bcmo1), a member of a ubiquitous family of carotenoid- and retinoid-modifying enzymes (*19*, *20*). Since mammalian Bcmo1 is expressed in a variety of tissues (*21*), carotenoid

† This work was supported by the Ministry of Science, Research and the Arts, Baden-Württemberg, and a grant of the German research foundation (DFG).

* To whom correspondence should be addressed: Institute of Biology I, Neurobiology and Animal Physiology, University of Freiburg, Hauptstrasse 1, D-79104 Freiburg, Germany. Telephone: +49 761 203 2539. Fax: +49 761 203 2921. E-mail: Johannes.von.Lintig@biologie.uni-freiburg.de.

‡ Present address: Renal Division, University Hospital of Freiburg, Hugstetter Strasse 55, D-79106 Freiburg, Germany.

§ Present address: Institute of Biology II, University of Freiburg, Schaenzlestrasse 1, D-79104 Freiburg im Breisgau, Germany.

10.1021/bi060701u CCC: $33.50
Published on Web 10/20/2006

transport mechanisms may also impact vitamin A-dependent processes in vision (mediated by 11-*cis*-retinal) and gene regulation (mediated by retinoic acid).

A relationship between class B scavenger receptor function and carotenoid transport was first suggested by genetic analysis in *Drosophila melanogaster* (*22*). The fly's *ninaD* gene encodes a SR-BI homologous protein, and disruption of its function causes blindness (*22*). In the study presented here, we further characterize the function of the fly's SR-BI homologue. We show that the two isoforms resulting from alternative splicing of *ninaD* mRNA are both membrane-bound proteins but are localized in different subcellular compartments. NinaD-I, the long isoform, is a cell surface receptor which can mediate uptake of carotenoid from micelles. We further demonstrate in vivo that NinaD-I plays a dual role in absorption and body distribution of dietary carotenoids. We also provide evidence that NinaD-I acts in vitamin E absorption like its mammalian counterpart. In contrast, cholesterol homeostasis was unaffected in *ninaD* mutants. Altogether, the evolutionary conservation of NinaD-I and SR-BI in the transport of fat soluble vitamins reveals a heretofore neglected link between class B scavenger receptor function and the numerous physiological roles exerted by these compounds in animal physiology.

EXPERIMENTAL PROCEDURES

Drosophila Maintenance, Fly Strains, and Crosses. Flies were reared on standard corn medium at 25 °C. The following *D. melanogaster* strains were used: $ninaB^{360d}$, $ninaD^{P245}$, Oregon R white, WTB (Berlin), and $ninaE^{17ol}$. For construction of *UAS-ninaD-I* flies, see ref *22*. $ninaD^{P245}/ninaD^{P245}$; tubP-GAL4/UAS-*ninaD-I* flies were obtained by crossing $ninaD^{P245}$ flies containing the *UAS-ninaD-I* transgene with #5138 (Bloomington *Drosophila* Stock Center, genotype, y^1w^*; P{tubP-GAL4}LL7/TM3, Sb^1). $ninaD^{P245}$/CyO, hsp70-GFP flies were obtained by crossing homozygous $ninaD^{P245}$ flies with #5702 (Bloomington *Drosophila* Stock Center, genotype, w^1; noc^{Sco}/CyO, P{GAL4-Hsp70.PB}TR1, P{UAS-GFP.Y}TR1).

Estimation of mRNA Levels by Semiquantitative RT-PCR Analyses. To analyze postembryonic *ninaD* and *ninaB* expression patterns, total RNA was isolated from staged wild-type animals. To attribute *ninaD* expression to different body parts, imagoes were hand-dissected into heads, thoraces, and abdomens. Total RNA was isolated with Trizol reagent (Invitrogen) according to the manufacturer's protocol. RNA samples were cleaned up and DNase-digested with the RNeasy Mini Kit (Qiagen). Reverse transcription was performed with Superscript II (Invitrogen) using an oligo-$(dT)_{17}$ primer. All cDNA preparations were made at one time to minimize variations in the reverse transcription reaction. The primers used for RT-PCR were intron-spanning. For *ninaD* RT-PCR, the following primers were used: forward, 5′-CTGGCCTGGCTTTATAGACTC-3′; and reverse, 5′-GCTATTCCGCATTTGGTTTGAAGC-3′. Primers were designed to amplify both *ninaD-I* and *ninaD-II* splice variants at the same time. For *ninaB* RT-PCR, the following primers were used: forward, 5′-GTGGTCACGGAGTTTGGCAC-3′; and reverse, 5′-TCCGTTAAGCCGAAGGTGTG-3′. *Drosophila* ribosomal protein *rp49* served as a control gene by utilizing the following primer set: forward, 5′-ATGAC-CATCCGCCCAGCATA-3′; and reverse, 5′-TACAAAT-GTGTATTCCGACCA-3′.

Northern Blot Analyses. Northern blot analyses were performed as described previously (*22*).

Extraction of Carotenoids and Retinoids and HPLC Analyses. Lipid compounds of flies were extracted as described previously (*22*). For extraction of Schneider S2 cells, cells were sonicated in 200 μL of PBS. For cells and media, hydroxylamine was omitted and otherwise extracted as described for flies. Carotenoids and tocopherols were analyzed and quantified by HPLC essentially as described in ref *23* with modifications. The column was developed at a constant flow rate of 1 mL/min with 0% A linear to 57% A in 45 min, and then to 0% B within 1 min, maintaining the final condition for an additional 14 min. Identification of tocopherols and quantification of tocopherol area units were achieved by chromatographic comparison with standard substances (Sigma).

For the assessment of carotenoids and retinoids, HPLC systems were as described previously (*22*). The HPLC solvent for quantification of xanthophylls was an *n*-hexane/diethyl ether/ethanol mixture (79/20/1, by volume). For β-carotene content determination, the HPLC solvent was an *n*-hexane/ethanol mixture (99.5/0.5, by volume).

Construction of S2 Cell Expression Vectors. For cloning of *ninaD-II*, the primers 5′-TGGGTACCAATATGTGCT-GCAGCTGCTGT-3′ (forward) and 5′-ATTCTCGAGCTC-TATAACGCTGTCTGGCTC-3′ (reverse) were used. *ninaD-I* was cloned using the same forward primer and the 5′-ATCCTCGAGAAAGTTTCGTTCGACCACGTTG-3′ reverse primer. For cloning of murine *SR-BI*, the forward primer was 5′-TAGGTACCGACATGGGCGGCAGCTCCA-3′ and the reverse primer was 5′-TTCTCGAGTAGCTTG-GCTTCTTGCAGCACC-3′. PCR products were cut with KpnI and XhoI and ligated into a likewise-treated pMT-V5/His A expression vector (Invitrogen). For construction of the mCD8-GFP expression vector, the fusion gene was amplified from a UAS-mCD8-GFP fly (Bloomington #5137) (*24*) in a single-fly PCR (*25*) using the following primer pair: forward, 5′-CTGCAACTACTGAAATCTGCC-3′; and reverse, 5′-GGCATTCCACCACTGCTCCC-3′. The PCR product was cut with XhoI and XbaI and ligated into a likewise-treated S2 cell expression vector pRmHa3 variant (*26*).

Cell Maintenance. S2 cells were purchased from Invitrogen and grown in Schneider's *Drosophila* medium (Invitrogen) containing 10% fetal bovine serum, 50 units of penicillin, and 50 μg/mL streptomycin, in 25 cm^2 cell culture flasks (Greiner bio-one). Cells were maintained at 28 °C.

Transient Transfection of S2 Cells and Induction. On the day prior to transfection, cells were seeded in cell culture dishes (Greiner bio-one). To ensure comparability, for each experiment a single pool of cells was used. Transient transfection was achieved using Cellfectin reagent (Invitrogen) according to the manufacturer's protocol. Protein expression was induced 24 h post-transfection by addition of 1 mM copper sulfate. Assays were carried out 48 h post-transfection.

Preparation of Media. Carotenoid-rich micellar media were prepared essentially as described previously (*27*). Carotenoids were dissolved in ethanol (for zeaxanthin) or *n*-hexane (for β-carotene) and dried under N_2. The residue

was reconstituted in Tween 40 and acetone (1/5, by volume) and again dried under N_2. This residue was dispersed with S2 medium (Invitrogen) containing serum and antibiotics by vortexing, giving final concentrations in the growth media of 1 mL of Tween 40/L and 5 μM carotenoid prior to sterile filtration unless noted otherwise. Media were sterile-filtered using Rotilabo 0.22 μm cellulose acetate filters (Roth).

Uptake of Carotenoid by S2 Cells. For the assay of carotenoid uptake, 4.5×10^6 cells were seeded in 60 mm cell culture dishes (Greiner bio-one). Transfection was accomplished with a total of 4 μg of *ninaD-I* expression vector, *ninaD-II* expression vector, or both, *mSR-BI* expression vector, or mCD8-GFP control vector (2 μg each). Where appropriate, an empty vector was used to deliver the same amounts of DNA. Cells received medium containing either zeaxanthin- or β-carotene-loaded micelles for 4 h. Average carotenoid concentrations in the medium after sterile filtration were as follows: 2.84 μM zeaxanthin and 0.86 μM β-carotene.

To determine zeaxanthin uptake kinetics, 1.5×10^6 cells were seeded in 30 mm culture dishes and transfected with 2 μg of *ninaD-I* or mCD8-GFP expression vector. Cells were harvested after different incubation times of up to 2 h. For each time point, a mCD8-GFP control was included. The zeaxanthin concentration after sterile filtration was 3.87 μM.

To assess the effect of concentration on the zeaxanthin uptake rate, 1.5×10^6 cells were seeded in 30 mm culture dishes and transfected with 2 μg of *ninaD-I* expression vector. Media with micellar zeaxanthin concentrations of up to 5 μM were prepared. Cells were incubated in these media for 40 min.

After incubation in carotenoid-rich media, cells were washed twice with PBS and Tween 40 and harvested by scraping. Protein concentrations were estimated using the Roti-Nanoquant Kit (Roth) according to the manufacturer's protocol.

Determination of Subcellular Localization of NinaD-I and NinaD-II. S2 cells were seeded in 30 mm cell culture dishes on top of poly-L-lysine (Sigma-Aldrich)-coated coverslips. Twenty-four hours after induction of protein expression, coverslips were washed with PBS and removed from the dishes. Cells were fixed with ice-cold methanol for 5 min. Methanol was removed, and 4% paraformaldehyde was added for 10 min. Cells were washed with PBST (PBS containing 0.1% Triton X-100) and blocked with PBSTM (PBST containing 1% skim milk powder, w/v) for 30 min at room temperature. Coverslips were incubated in PBSTM containing anti-V5 antibody (1/200) (Invitrogen) overnight at 4 °C, washed three times with PBSTM, and incubated in anti-mouse Cy3 antibody (1/200) (Jackson ImmunoResearch) for 1 h at room temperature. Following three washes with PBS, coverslips were mounted on microscope slides with Vectashield mounting medium containing DAPI. Fluorescence signals were recorded on a Zeiss Axiophot epifluorescence microscope. Confocal laser scanning microscopy was carried out with a Leica TCS4D microscope.

For discrimination of soluble and membrane-bound fractions, transiently transfected S2 cells expressing *ninaD-I* or *ninaD-II* were sonicated in PBS containing Complete-Mini protease inhibitors (Roche Applied Science) and centrifuged for 5 min at 16000*g*. Supernatants were ultracentrifuged at 100000*g* for 1 h at 4 °C. Pellets and supernatants from ultracentrifugation were subjected to Western blot analysis.

Western Blot Analyses. For Western blot analysis of fly heads, 10 heads were hand dissected, homogenized in SDS buffer, and incubated at room temperature for 5 min. Proteins were separated by SDS−polyacrylamide gel electrophoresis and blotted to a nitrocellulose membrane. The primary antibody was the mouse monoclonal anti-Rh1 antibody (4C5 concentrate, Hybridoma Bank) (1/1000). The secondary antibody was the peroxidase-conjugated anti-mouse antibody (Sigma). Staining was accomplished with ECL Western blotting detection reagents (Amersham Biosciences). S2 cells or ultracentrifuged fractions were homogenized in SDS buffer and incubated at 100 °C for 5 min and otherwise treated in the same manner as fly heads. Mouse monoclonal IgG_{2a} anti-V5 antibody (Invitrogen) was used as primary antibody (1/5000). The secondary antibody was the peroxidase-conjugated anti-mouse Ig antibody (Sigma).

Sterol Determination by Gas Chromatography and Mass Spectrometry (GC−MS). For quantitative and qualitative sterol determination, 10 flies were homogenized in Trizin buffer (50 mM Trizin and 100 mM NaCl) and extracted three times with a chloroform/methanol mixture (1/1, by volume). GC−MS analyses were carried out on a Hewlett-Packard 6890 gas chromatograph. For mass spectrometry, a Hewlett-Packard 5973 device (70 eV) was used.

RESULTS

The Two NinaD Protein Variants Are Localized in Different Subcellular Compartments. Two splicing variants are expressed from the *ninaD* gene (*22*). Here, we term the resulting proteins NinaD-I and NinaD-II. Structural predictions revealed that NinaD-I possesses two putative transmembrane domains, near its N- and C-termini, whereas NinaD-II lacks the C-terminal region of NinaD-I, including the putative transmembrane region, but is otherwise identical to NinaD-I (Figure 1A). To assess the subcellular localization of the two NinaD proteins, we expressed each as a V5-tagged form in transiently transfected *Drosophila* Schneider S2 cells and performed immunocytochemistry. Epifluorescence and confocal microscopy revealed that NinaD-I was located at the plasma membrane (Figure 1B,D). In contrast, NinaD-II was located intracellularly in a network-like pattern excluding the nucleus, but with no detectable staining of the plasma membrane (Figure 1C,E). To verify that both NinaD protein isoforms were associated with membranes, transiently transfected S2 cells expressing each of the NinaD isoforms were disrupted, and soluble and membranous fractions were separated by ultracentrifugation. Western blot analysis confirmed that both NinaD variants were enriched in the pellets containing the membrane fractions (Figure 1F).

NinaD-I Is a Cell Surface Receptor that Can Mediate the Cellular Uptake of Carotenoids from Micelles. To elucidate the roles of the NinaD protein variants in uptake of carotenoids into target cells, we established an in vitro test system. For this purpose, we transiently transfected S2 cells with different expression vector constructs. S2 cells expressing mCD8-GFP, a membrane-bound GFP fusion protein, were used as a control. First, we confirmed *ninaD-I* and *-II* expression in transfected S2 cells by Western blot analysis (Figure 2A). Cells were incubated with medium containing

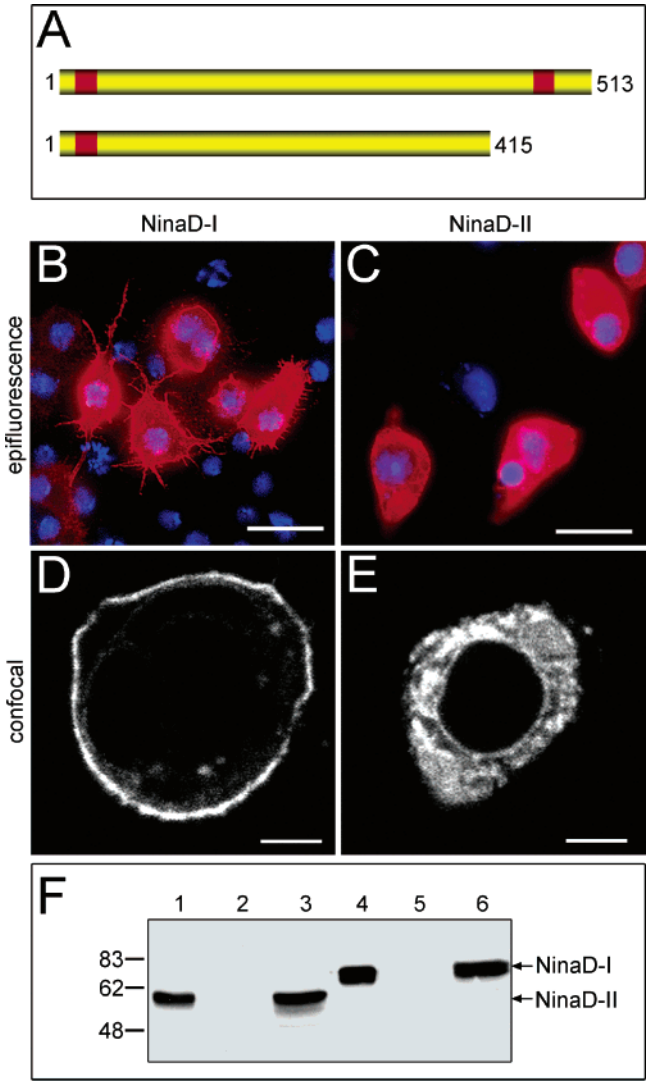

FIGURE 1: Subcellular localization of NinaD-I and NinaD-II. (A) Primary structures of the two NinaD protein isoforms. Predicted transmembrane domains are denoted with red boxes. Both NinaD-I (top schematic) and NinaD-II (bottom schematic) contain a putative N-terminal transmembrane domain of ~21 amino acids that is located ~15 amino acids from the N-terminus. NinaD-I contains an additional predicted transmembrane domain comprising ~20 amino acids that is located ~36 residues from the C-terminus. Thus, NinaD-I contains a putative extracellular domain comprising ~421 residues. (B−E) Immunocytochemistry of transiently transfected S2 cells expressing *ninaD-I* (B and D) or *ninaD-II* (C and E). Panels B and C show epifluorescence images showing labeling of recombinantly expressed NinaD-I or NinaD-II, which was detected with an antibody raised against the V5 epitope of the proteins and Cy3-conjugated secondary antibody (red), and cell nuclei stained with DAPI (blue). Scale bars are 10 μm. Panels D and E show confocal images depicting the immunofluorescence labeling of NinaD-I and NinaD-II in one optical section that is approximately 0.26 μm thick. Scale bars are 2.5 μm. (F) Western blot analysis detecting V5 epitope-tagged NinaD-I and NinaD-II proteins in cell homogenates before and after ultracentrifugation (UC): lane 1, lysates of *ninaD-II*-expressing cells prior to UC; lane 2, *ninaD-II* supernatant after UC; lane 3, *ninaD-II* pellet after UC; lane 4, lysates of *ninaD-I*-expressing cells prior to UC; lane 5, *ninaD-I* supernatant after UC; and lane 6, *ninaD-I* pellet after UC. The pellet contains the membrane fraction, and the soluble fraction is in the supernatant. Molecular mass markers (in kilodaltons) are indicated at the left.

zeaxanthin-loaded Tween 40 micelles. After 4 h, the carotenoid contents of the cells were determined by quantitative HPLC analysis. S2 cells expressing *ninaD-I* accumulated 7.6-fold larger amounts of zeaxanthin, as compared to controls expressing mCD8-GFP (Figure 2B). In cells expressing *ninaD-II*, no significant increase in zeaxanthin content was observed as compared to controls. Coexpression of both *ninaD-I* and *ninaD-II* led to zeaxanthin contents which were 6.2-fold higher than that of mCD8-GFP-expressing controls with rather high interexperiment variations (Figure 2B). A similar result was obtained when β-carotene-loaded Tween 40 micelles were used (Figure 2C). However, even though overall β-carotene uptake was slower than zeaxanthin uptake, this pure hydrocarbon accumulated to an extent 18.3-fold greater in *ninaD-I*-expressing cells than in control levels. Additionally, it must be noted that, consistent with the results of O'Sullivan et al. (*27*), the β-carotene concentration in micelle preparations was considerably lower than the zeaxanthin concentration (see Experimental Procedures).

To analyze the kinetics of uptake of zeaxanthin by NinaD-I, we incubated S2 cells expressing *ninaD-I* or mCD8-GFP for different periods of time with medium containing zeaxanthin-loaded micelles. Carotenoid uptake leveled out at longer incubation time in both cell lines, but the rate was significantly higher in *ninaD-I*-expressing cells (Figure 2D).

Additionally, we varied the zeaxanthin content of the micelles to investigate the concentration dependency of the zeaxanthin uptake rate (Figure 2E). The rate of zeaxanthin uptake increased linearly in the range of 0.07−1.7 μM and plateaued at higher concentrations (1.7−3.6 μM). In summary, NinaD-I-mediated carotenoid uptake from micelles was found to be concentration-dependent and saturable.

Recently, it has been shown that SR-BI mediates the cellular uptake of carotenoids (*15*, *16*). Therefore, we expressed murine SR-BI in our test system. As shown in Figure 2F, the murine homologue, like NinaD-I, efficiently mediated uptake of zeaxanthin into S2 cells.

NinaD Exerts a Dual Role in the Absorption and Body Distribution of Dietary Carotenoids. We have previously shown that *ninaD* is already expressed embryonically in the gut primordium and in adipocytes (*22*). To analyze post-embryonic *ninaD* mRNA expression patterns, we performed semiquantitative RT-PCR analyses using staged wild-type animals. Primers for RT-PCR were designed to detect a region shared by both *ninaD* splice variants, thus resulting in a single band for total *ninaD*. We found abundant *ninaD* mRNA levels in third instar larvae, late pupae, and young imagoes (Figure 3A, top panel). In the latter, *ninaD* mRNA expression could be localized to heads, thoraces, and abdomens (Figure 3B). Northern blot analysis revealed that both variants are expressed in comparable amounts in heads as well as bodies of wild-type imagoes (Figure 3C). We also determined mRNA levels of *ninaB*, which encodes Bcmo1, the enzyme catalyzing the subsequent step in the conversion of dietary carotenoids to retinoids (*28*, *29*). High *ninaB* expression levels were detectable in late pupae and young imagoes (Figure 3A, middle panel), when visual pigments are synthesized in the developing compound eyes.

To correlate temporal and spatial *ninaD* expression with carotenoid levels, we performed HPLC analyses (Figure 4A, top panel). Since homozygous $ninaD^{P245}$ flies cannot be propagated due to male sterility and the heterozygous marker CyO can only be detected in imagoes, we first generated a heterozygous $ninaD^{P245}$/CyO, hsp70-GFP fly strain. Heterozygous offspring of this strain can be discriminated from

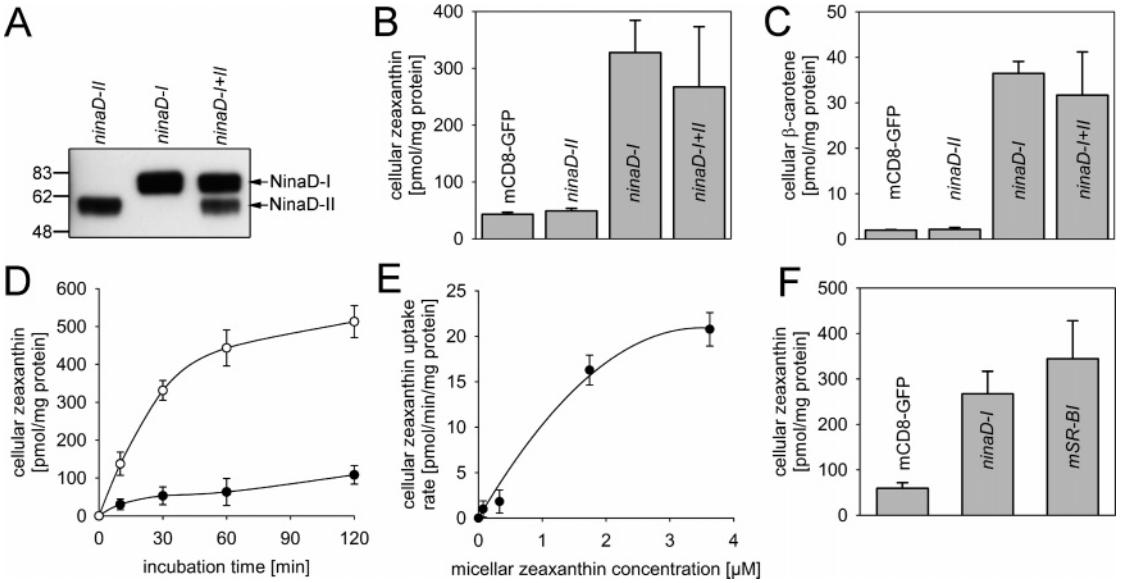

FIGURE 2: NinaD-I mediates uptake of zeaxanthin and β-carotene into S2 cells. (A) Western blot analysis of transiently transfected S2 cells expressing *ninaD-I* and *ninaD-II*. Assessment of protein levels was accomplished using an antibody raised against the V5 tag introduced into the proteins. Molecular mass markers (in kilodaltons) are indicated at the left. (B) Zeaxanthin uptake by transiently transfected S2 cells from loaded micelles after 4 h. Cells were transfected with 2 μg of expression vectors as indicated. Note that, where appropriate, cells were transfected with empty vector to deliver the same amounts of DNA (see Experimental Procedures). Bars indicate averages from three independent experiments. (C) Uptake of β-carotene by transiently transfected S2 cells. Bars indicate results obtained from three independent experiments. (D) Time course of uptake of cellular zeaxanthin into S2 cells: (○) *ninaD-I*-expressing cells and (●) mCD8-GFP-expressing control cells. Results from triplicate determinations are shown. (E) Effect of micellar zeaxanthin concentration on cellular zeaxanthin uptake rate. The incubation time was 40 min. Error bars indicate standard deviations obtained from triplicate determinations. (F) Uptake of zeaxanthin by transiently transfected S2 cells expressing murine *SR-BI*. Experimental conditions were the same as in panel B. The diagram shows that mSR-BI-mediated cellular zeaxanthin uptake. Bars indicate averages from triplicate determinations. Note that experimental conditions in panels D and E were different from those in panels B, C, and F (see Experimental Procedures).

their homozygous siblings at larval stages by expression of green fluorescent protein (GFP). We found that homozygous *ninaD*^{P245} third instar larvae contained only 2.7% of the carotenoid content of heterozygous siblings. Since carotenoids must be acquired during this stage for subsequent metamorphosis, *ninaD*^{P245} pupae also exhibited dramatically decreased carotenoid contents as compared to heterozygous siblings. In *ninaD*^{P245} imagoes, the carotenoid content was even further reduced, while heterozygous flies still contained considerable amounts. Additionally, the chromophore 3-hydroxyretinal was readily formed in heterozygotes, while it was not detectable in homozygous *ninaD*^{P245} imagoes (data not shown). To analyze the body distribution of carotenoids, we took advantage of the *ninaB* mutant, which is impaired in conversion of carotenoids to retinoids (*29*). As shown in Figure 4B, *ninaB* imagoes exhibited a significant accumulation of carotenoids as compared to controls. Interestingly, carotenoids mainly accumulated in heads, consistent with *ninaB* expression in this part of the body (*29*). Thus, carotenoid levels and body distribution mirrored spatiotemporal mRNA expression patterns of both the *ninaD* and *ninaB* genes.

ninaD Flies Exhibit Decreased α*-Tocopherol Levels.* In mammals, SR-BI has been shown to be involved in several aspects of lipid metabolism, such as cholesterol and vitamin E transport (*30*). Therefore, we also determined sterol levels in homozygous and heterozygous *ninaD* flies. However, we found no qualitative and quantitative differences in the sterol composition by GC−MS analysis (data not shown). This excludes a significant contribution of NinaD in sterol absorption. However, *Drosophila*, like other insects, does not produce this substance by an endogenous biochemical

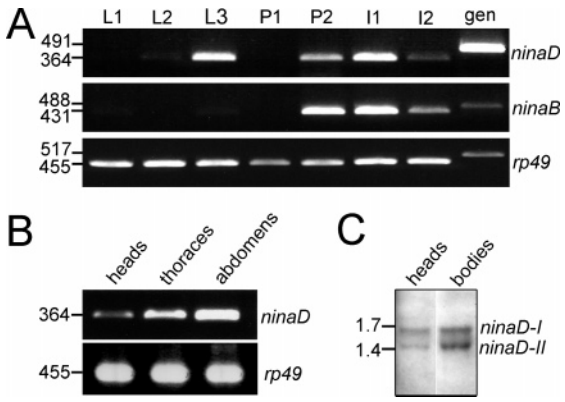

FIGURE 3: Temporal and spatial expression patterns of *ninaD* are in accordance with NinaD function. (A) Semiquantitative RT-PCR showing the temporal postembryonic expression patterns of *ninaD* and *ninaB* mRNA: L1−L3, first to third instar larvae, respectively; P1 and P2, early and late pupae, respectively; I1, 1−2 days post-eclosion (dpe) imagoes; I2, >10 dpe imagoes; gen, genomic DNA used as a PCR template that resulted in larger amplification products due to usage of intron-spanning primers. High *ninaD* transcript abundance was detected in third instar larvae, late pupae, and young imagoes. A prominent *ninaB* signal was detected in P2, I1, and I2. Expected sizes of PCR products (in base pairs) from cDNA and genomic templates are indicated at the left. *ninaD* primers were designed for detection of both *ninaD-I* and *-II* transcripts at the same time, resulting in a single band. (B) Semiquantitative RT-PCR of heads, thoraces, and abdomens of wild-type imagoes shows that *ninaD* is expressed in all three body parts. Ribosomal protein 49 (*rp49*) served as a control gene because of its abundant expression regardless of the developmental stage or body part. Expected sizes of PCR products (in base pairs) are indicated at the left. (C) Northern blot analyses of wild-type fly heads and bodies showing that both *ninaD* splice variants are present in different body parts. Size markers (in kilobases) are indicated at the left.

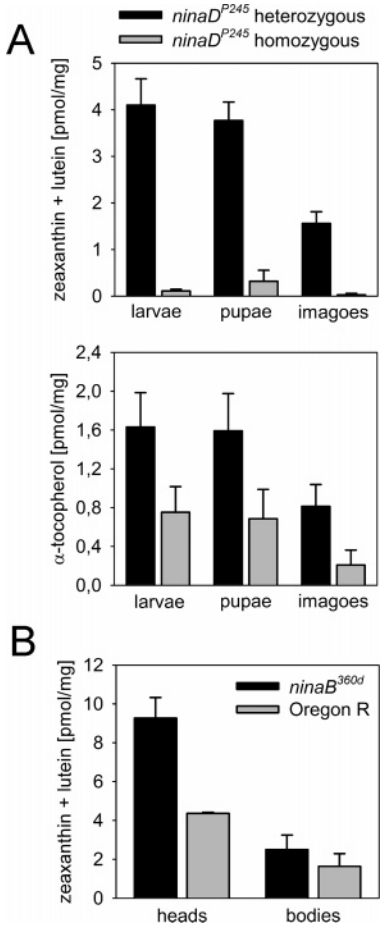

FIGURE 4: (A) *ninaD* mutant flies exhibit reduced carotenoid and α-tocopherol levels throughout development. Lipid components were extracted from third instar larvae, pupae, and imagoes of homozygous and heterozygous *ninaD*^{P245} mutants and subjected to HPLC analyses. The top panel shows that the lutein + zeaxanthin contents are drastically reduced in homozygous *ninaD* mutants throughout development. Heterozygous *ninaD* mutants harboring one functional *ninaD* allele contained considerable amounts of carotenoids. Bars indicate averages of four independent experiments. The bottom panel shows that homozygous *ninaD* mutants contained lower α-tocopherol levels than heterozygous control animals at all stages that were examined. Bars indicate averages of three independent experiments. (B) The *ninaB* mutation leads to a significant accumulation of carotenoids in the head. Heads and bodies of *ninaB*^{360d} and wild-type control (Oregon R white) imagoes were separated. Lipid compounds were extracted and subjected to HPLC analysis. Bars indicate averages obtained from three independent experiments.

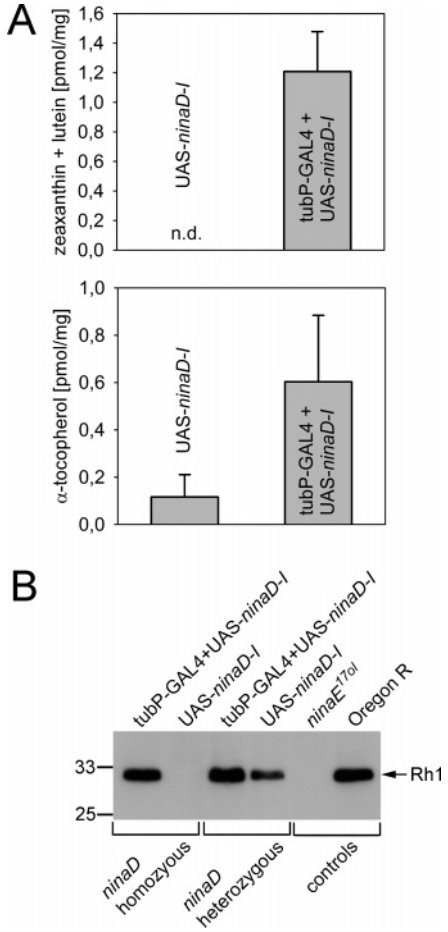

FIGURE 5: Carotenoid and vitamin E deficiency of *ninaD* flies can be rescued by ectopic expression of a *ninaD-I* transgene (UAS-*ninaD-I*) under the control of a *tubulin* (tubP-GAL4) driver. (A) Lipid extracts from flies expressing a *ninaD-I* transgene (tubP-GAL4 + UAS-*ninaD-I*) and controls not expressing the transgene (UAS-*ninaD-I*) in a *ninaD* mutant background were analyzed by HPLC analysis. As shown in the top panel, transgene expression restored carotenoid levels whereas no carotenoids were detectable in controls. The bottom panel shows that transgene expression led to increased α-tocopherol contents as compared to control flies. Bars represent averages of three independent crossing experiments. (B) Western blot analysis assessing Rh1 contents in heads of all offspring strains obtained from the rescue crossing. Homozygous *ninaD* flies contained rhodopsin only when the *ninaD-I* transgene was expressed under the control of a *tubulin* driver. Heterozygous flies contained rhodopsin irrespective of transgene expression. *ninaE*^{17o1} (rhodopsin null) and Oregon R flies served as negative and positive controls, respectively. Molecular mass markers (in kilodaltons) are indicated at the left.

pathway and, thus, strictly depends on dietary cholesterol supply (*31*). We then determined the tocopherol content of the flies by HPLC analysis. We found α-tocopherol to be the major derivative in *Drosophila*, while other derivatives such δ- and γ-tocopherol were detectable in only trace amounts. As shown in Figure 4A, homozygous *ninaD* flies exhibited reduced levels of α-tocopherol at larval (0.75 vs 1.63 pmol/mg) and pupal (0.69 vs 1.59 pmol/mg) stages, and the level further decreased in young imagoes (0.21 vs 0.81 pmol/mg) as compared to heterozygous controls.

Carotenoid and Vitamin E Deficiency of ninaD Mutant Flies Can Be Rescued by Ectopic Expression of ninaD-I. We found that NinaD-I, the longer NinaD variant, is sufficient to mediate uptake of carotenoid into S2 cells. To provide in vivo evidence for this function, we used a fly strain harboring a wild-type *ninaD-I* transgene (*22*). By appropriate crossings, we established a fly strain expressing UAS-*ninaD-I* under the control of a *tubulin*-GAL4 driver in a *ninaD*^{P245} mutant genetic background. We used *ninaD* flies harboring solely the UAS-*ninaD-I* transgene as controls. As expected, the carotenoid content of imagoes expressing the transgene was highly elevated (Figure 5A, top panel), showing that ubiquitous expression of *ninaD-I* is sufficient to rescue the defect in carotenoid absorption. To show that ectopic expression of *ninaD-I* not only restores absorption of dietary carotenoids but also rescues blindness of *ninaD* mutants, we performed a Western blot analysis for Rh1 (Figure 5B). Rh1 is the major visual pigment in *Drosophila*, and its biogenesis is strictly dependent on the availability of the visual chromophore, 3-hydroxyretinal (*32*). The detection of Rh1 proved that carotenoids acquired by ectopic expres-

sion of *ninaD-I* were readily used for visual pigment synthesis. No Rh1 could be detected in *ninaD* mutants harboring the UAS-*ninaD-I* transgene alone, confirming that the system was not permissive for transgene expression when the GAL4 driver is absent.

Since *ninaD* mutants also exhibited decreased vitamin E levels, we determined tocopherol contents in *ninaD* mutant flies expressing the UAS-*ninaD-I* transgene (Figure 5A, bottom panel). We found that α-tocopherol contents were restored to control levels (see Figure 4A, bottom panel), providing in vivo evidence for the involvement of NinaD-I in vitamin E metabolism.

DISCUSSION

We have previously shown that the *ninaD* gene encodes two protein variants, which we termed here NinaD-I and -II. For further characterization, we expressed both of them in *Drosophila* S2 cells. Immunocytochemistry showed that NinaD-I was localized at the plasma membrane, whereas NinaD-II was localized intracellularly. Both variants were detectable in the membrane fraction in Western blot analyses. Consistent with the subcellular localization, we found that only NinaD-I can mediate the cellular uptake of carotenoids from micelles. Thus, a direct interaction between NinaD-I, which is localized at the plasma membrane, and micelles seems to be crucial for rendering carotenoids available from these micelles. We also showed that NinaD-I-mediated cellular uptake of zeaxanthin was concentration-dependent and saturable.

Recently, it has been shown that mammalian SR-BI can mediate the uptake of carotenoids (lutein and β-carotene) from micelles (*15*, *16*). Therefore, we asked whether SR-BI functions also in S2 cells, e.g., to mediate zeaxanthin uptake. Indeed, SR-BI performed this task, and zeaxanthin accumulated to an extent comparable to that in NinaD-I-expressing S2 cells, thus further validating our test system. Flies can use both zeaxanthin and β-carotene for the synthesis of the visual chromophore 3-hydroxyretinal (*33*, *34*). We found that overall cellular uptake rates for zeaxanthin were much higher than those of β-carotene. There are different possible explanations for this finding. First, the β-carotene concentration in micelles after sterile filtration was lower than the zeaxanthin concentration (see Experimental Procedures). Second, this difference might be explained by a higher specificity of NinaD-I for zeaxanthin. Third, zeaxanthin availability for NinaD-I from micelles might be better than that of β-carotene. We suppose that the last assumption is more likely valid since β-carotene was enriched in NinaD-I-expressing cells to an even higher extent than zeaxanthin. Additionally, the higher cellular levels of zeaxanthin might be explained by intracellular factors, e.g., binding proteins or other sequestration mechanisms, which might contribute to the accumulation of this xanthophyll.

The efficient rescue of the carotenoid-deficient phenotype and blindness of *ninaD* mutants by ectopic expression of a *ninaD-I* transgene driven by a strong ubiquitously active promoter proved its functional significance. While all these results show both in vitro and in vivo that NinaD-I plays a crucial role in carotenoid transport processes, the function of the second protein variant, NinaD-II, remains elusive. Interestingly, a protein variant of the mammalian scavenger receptor SR-BI, called SR-BII, exists in mammals, resulting from alternative splicing. Like NinaD-II, SR-BII is mainly located at intracellular membranes and differs from SR-BI in its C-terminal region. SR-BII has been suggested to play a role in the endocytosis of lipoprotein particles into target cells (*35*, *36*). It remains to be elucidated whether NinaD-II might play a comparable role in lipoprotein-mediated lipid metabolism in insects.

Embryonically, *ninaD* is expressed in the gut primordia and adipocytes (*22*). Here, we show that postembryonically, *ninaD* is expressed during third larval instar, late pupal, and imago stages of the *Drosophila* life cycle. The third instar larval stage is characterized by a high level of intake and storage of dietary lipids to promote metamorphosis. A recent study reports the upregulation of a gene promoting fat storage in third instar *Drosophila* larvae (*37*). Upregulation of *ninaD* mRNA levels at this stage therefore indicates that NinaD plays a role in the absorption of dietary carotenoids. We obtained direct evidence of this inference by showing that the carotenoid contents of $ninaD^{P245}$ larvae and pupae are drastically reduced compared to those of their heterozygous siblings. Furthermore, as already mentioned, we found that NinaD-I can mediate uptake of carotenoid from artificial micelles in a cell culture test system, indicating that carotenoid absorption is a regulated protein-mediated process, as proposed for vertebrates (*15*, *16*). In the latter, SR-BI not only functions in the gut but also plays an important role in lipoprotein-mediated lipid metabolism (*8*−*11*). For the exchange of cholesterol with HDL, a direct interaction between SR-BI and the HDL apoprotein moiety has been demonstrated (*7*). In insects, carotenoids are transported in lipophorins, which are structurally related to mammalian lipoprotein particles (*38*). Since *ninaD* mRNA levels rose again at late pupal stages, temporally coinciding with expression of *ninaB* and visual pigment formation, NinaD-I may also function in lipophorin-mediated body distribution of lipids. Previously, we provided in vivo evidence that this is the case by demonstrating that ectopic expression of *ninaD-I* in photoreceptor cells led to an increase in the carotenoid content of the heads above control levels (*22*). Additionally, analysis of *ninaB* imagoes showed that carotenoids accumulated in the flies' heads, indicating that carotenoids are transported from larval stores to *ninaB*-expressing cells for conversion to retinoids, a process which is impaired in this mutant.

In contrast to our study, Gu and co-workers recently suggested that NinaD and NinaB act within a certain neuronal cell type in the central nervous system to produce retinal from β-carotene (*39*). It is noteworthy that these authors used the $ninaD^{P246}$ mutant strain, which has yet not been molecularly characterized. For our studies, we used the $ninaD^{P245}$ strain carrying a nonsense mutation which causes a premature termination of translation of both NinaD protein variants (*22*). Furthermore, these authors did not combine their genetic studies, e.g., the ectopic expression of *ninaD*, with detailed biochemical analyses of carotenoid and retinoid contents as we did here. Thus, while there might be various explanations for the discrepancy between both studies, the most plausible is that the $ninaD^{P246}$ mutation affects carotenoid metabolism at a level different from that of the $ninaD^{P245}$ mutation.

Vogt and Kirschfeld (*33*) as well as Giovannucci and Stephenson (*34*) reported that zeaxanthin is the storage and

transport form for carotenoids in *Calliphora* and *Drosophila*, respectively. Additionally, these authors showed that dietary β-carotene is hydroxylated to yield zeaxanthin in flies. In our analysis, we exclusively found zeaxanthin and lutein, but no β-carotene, in flies even though besides xanthophylls, as major constituents, the standard *Drosophila* diet contains this pure hydrocarbon (*22*). Thus, the finding of a metabolic transformation of β-carotene to zeaxanthin as well as the accumulation of xanthophylls in *ninaB* mutant flies (this study) strongly indicates that carotenoids hydroxylated at positions 3 and 3′ of the β-ionone ring are the direct precursors for 3-hydroxyretinal, the visual chromophore. This is also in accordance with our finding that zeaxanthin, when applied as the sole dietary carotenoid, can be readily used for 3-hydroxyretinal synthesis (data not shown). It remains to be shown that NinaB/Bcmo1, besides cleaving β-carotene (*28*), also catalyzes xanthophyll conversion in vitro. Additionally, our study provides evidence that NinaD-I and NinaB act sequentially in the visual chromophore biosynthetic pathway. Hereby, NinaD-I plays a dual role in carotenoid transport, first in rendering dietary carotenoids available in the third instar larval stage and second for distributing acquired carotenoids, most probably in the form of xanthophylls, to *ninaB*-expressing cells.

SR-BI plays an important role in the metabolism of additional isoprenoid compounds such as tocopherols and cholesterol (*30*). Indeed, we found that NinaD functions are not restricted to carotenoids but may also contribute to tocopherol metabolism. α-Tocopherol levels were reduced in *ninaD* mutants during all developmental stages, most pronouncedly in imagoes. However, this reduction was smaller than that of carotenoids, indicating that additional uptake mechanisms for tocopherols may exist in *Drosophila*. Additionally, we found α-tocopherol as a major vitamin E derivative, while other derivatives were only present in trace amounts. This finding cannot be explained by the composition of the diet since corn meal contains, besides α-tocopherol, other derivatives thereof in large quantities (*40*). In mammals, a specific α-tocopherol transfer protein (TTP) contributes to enrichment of α-tocopherol in the body. However, the mechanism for selective accumulation of α-tocopherol in *Drosophila* seems to be different from that in mammals involving cytochrome P_{450} tocopherol ω-hydroxylase-mediated catabolism of other tocopherol derivatives (*41*).

Impairments of sterol metabolism are fatal for flies which has recently been shown by mutagenesis of the NPC1 gene (*42*). Indeed, we found no evidence of the involvement of NinaD in the uptake of dietary sterols. Additionally, fundamental differences in the regulation of sterol metabolism between sterol auxotrophic insects and mammals exist; e.g., SREBP, the sensor for intracellular cholesterol levels in mammals, also exists in *Drosophila* but binds palmitate and senses fatty acid levels instead of cholesterol levels to maintain membrane structure and integrity (*43*).

In summary, our study reveals an evolutionarily conserved role of NinaD-I and SR-BI in the uptake and transport of carotenoids. In *Drosophila*, NinaD-I promotes the synthesis of 3-hydroxyretinal to establish vision, the only known role of retinoids in insects. In mammals, including humans, carotenoid derivatives function in vision and gene regulation (*44*). Since most animals, including humans, rely on carotenoids as the major source of vitamin A, the connection between class B scavenger receptor and vitamin A functions deserves further research.

ACKNOWLEDGMENT

We thank Drs. Randall Cassada and Vitus Oberhauser for helpful comments on the manuscript.

REFERENCES

1. Chawla, A., Repa, J. J., Evans, R. M., and Mangelsdorf, D. J. (2001) Nuclear receptors and lipid physiology: Opening the X-files, *Science 294*, 1866−1870.
2. Brewer, H. B., Jr., and Santamarina-Fojo, S. (2003) New insights into the role of the adenosine triphosphate-binding cassette transporters in high-density lipoprotein metabolism and reverse cholesterol transport, *Am. J. Cardiol. 91*, 3E−11E.
3. Hauser, H., Dyer, J. H., Nandy, A., Vega, M. A., Werder, M., Bieliauskaite, E., Weber, F. E., Compassi, S., Gemperli, A., Boffelli, D., Wehrli, E., Schulthess, G., and Phillips, M. C. (1998) Identification of a Receptor Mediating Absorption of Dietary Cholesterol in the Intestine, *Biochemistry 37*, 17843−17850.
4. Davis, H. R., Jr., Zhu, L. J., Hoos, L. M., Tetzloff, G., Maguire, M., Liu, J., Yao, X., Iyer, S. P., Lam, M. H., Lund, E. G., Detmers, P. A., Graziano, M. P., and Altmann, S. W. (2004) Niemann-Pick C1 Like 1 (NPC1L1) is the intestinal phytosterol and cholesterol transporter and a key modulator of whole-body cholesterol homeostasis, *J. Biol. Chem. 279*, 33586−33592.
5. Acton, S., Rigotti, A., Landschulz, K. T., Xu, S., Hobbs, H. H., and Krieger, M. (1996) Identification of scavenger receptor SR-BI as a high density lipoprotein receptor, *Science 271*, 518−520.
6. Landschulz, K. T., Pathak, R. K., Rigotti, A., Krieger, M., and Hobbs, H. H. (1996) Regulation of scavenger receptor, class B, type I, a high density lipoprotein receptor, in liver and steroidogenic tissues of the rat, *J. Clin. Invest. 98*, 984−995.
7. Xu, S., Laccotripe, M., Huang, X., Rigotti, A., Zannis, V. I., and Krieger, M. (1997) Apolipoproteins of HDL can directly mediate binding to the scavenger receptor SR-BI, an HDL receptor that mediates selective lipid uptake, *J. Lipid Res. 38*, 1289−1298.
8. Temel, R. E., Trigatti, B., DeMattos, R. B., Azhar, S., Krieger, M., and Williams, D. L. (1997) Scavenger receptor class B, type I (SR-BI) is the major route for the delivery of high density lipoprotein cholesterol to the steroidogenic pathway in cultured mouse adrenocortical cells, *Proc. Natl. Acad. Sci. U.S.A. 94*, 13600−13605.
9. Ji, Y., Jian, B., Wang, N., Sun, Y., Moya, M. L., Phillips, M. C., Rothblat, G. H., Swaney, J. B., and Tall, A. R. (1997) Scavenger receptor BI promotes high density lipoprotein-mediated cellular cholesterol efflux, *J. Biol. Chem. 272*, 20982−20985.
10. Jian, B., de la Llera-Moya, M., Ji, Y., Wang, N., Phillips, M. C., Swaney, J. B., Tall, A. R., and Rothblat, G. H. (1998) Scavenger receptor class B type I as a mediator of cellular cholesterol efflux to lipoproteins and phospholipid acceptors, *J. Biol. Chem. 273*, 5599−5606.
11. Glomset, J. A. (1968) The plasma lecithin:cholesterol acyltransferase reaction, *J. Lipid Res. 9*, 155−167.
12. Goti, D., Hrzenjak, A., Levak-Frank, S., Frank, S., van der Westhuyzen, D. R., Malle, E., and Sattler, W. (2001) Scavenger receptor class B, type I is expressed in porcine brain capillary endothelial cells and contributes to selective uptake of HDL-associated vitamin E, *J. Neurochem. 76*, 498−508.
13. Kolleck, I., Schlame, M., Fechner, H., Looman, A. C., Wissel, H., and Rustow, B. (1999) HDL is the major source of vitamin E for type II pneumocytes, *Free Radical Biol. Med. 27*, 882−890.
14. Reboul, E., Klein, A., Bietrix, F., Gleize, B., Malezet-Desmoulins, C., Schneider, M., Margotat, A., Lagrost, L., Collet, X., and Borel, P. (2006) Scavenger Receptor Class B Type I (SR-BI) is involved in Vitamin E Transport across the Enterocyte, *J. Biol. Chem. 281*, 4739−4745.
15. Reboul, E., Abou, L., Mikail, C., Ghiringhelli, O., Andre, M., Portugal, H., Jourdheuil-Rahmani, D., Amiot, M. J., Lairon, D., and Borel, P. (2005) Lutein transport by Caco-2 TC-7 cells occurs partly by a facilitated process involving the scavenger receptor class B type I (SR-BI), *Biochem. J. 387*, 455−461.
16. van Bennekum, A., Werder, M., Thuahnai, S. T., Han, C. H., Duong, P., Williams, D. L., Wettstein, P., Schulthess, G., Phillips,

M. C., and Hauser, H. (2005) Class B scavenger receptor-mediated intestinal absorption of dietary β-carotene and cholesterol, *Biochemistry 44*, 4517−4525.
17. Wald, G. (1945) Human Vision and the Spectrum, *Science 101*, 653−658.
18. Bone, R. A., Landrum, J. T., and Tarsis, S. L. (1985) Preliminary identification of the human macular pigment, *Vision Res. 25*, 1531−1535.
19. von Lintig, J., and Vogt, K. (2004) Vitamin A formation in animals: Molecular identification and functional characterization of carotene cleaving enzymes, *J. Nutr. 134*, 251S−256S.
20. von Lintig, J., Hessel, S., Isken, A., Kiefer, C., Lampert, J. M., Voolstra, O., and Vogt, K. (2005) Towards a better understanding of carotenoid metabolism in animals, *Biochim. Biophys. Acta 1740*, 122−131.
21. Lindqvist, A., and Andersson, S. (2002) Biochemical properties of purified recombinant human β-carotene 15,15′-monooxygenase, *J. Biol. Chem. 277*, 23942−23948.
22. Kiefer, C., Sumser, E., Wernet, M. F., and Von Lintig, J. (2002) A class B scavenger receptor mediates the cellular uptake of carotenoids in *Drosophila*, *Proc. Natl. Acad. Sci. U.S.A. 99*, 10581−10586.
23. Hoa, T. T., Al-Babili, S., Schaub, P., Potrykus, I., and Beyer, P. (2003) Golden Indica and Japonica Rice Lines Amenable to Deregulation, *Plant Physiol. 133*, 161−169.
24. Lee, T., Lee, A., and Luo, L. (1999) Development of the *Drosophila* mushroom bodies: Sequential generation of three distinct types of neurons from a neuroblast, *Development 126*, 4065−4076.
25. Gloor, G. B., Preston, C. R., Johnson-Schlitz, D. M., Nassif, N. A., Phillis, R. W., Benz, W. K., Robertson, H. M., and Engels, W. R. (1993) Type I repressors of P element mobility, *Genetics 135*, 81−95.
26. Bunch, T. A., Grinblat, Y., and Goldstein, L. S. (1988) Characterization and use of the *Drosophila* metallothionein promoter in cultured *Drosophila melanogaster* cells, *Nucleic Acids Res. 16*, 1043−1061.
27. O'Sullivan, S. M., Woods, J. A., and O'Brien, N. M. (2004) Use of Tween 40 and Tween 80 to deliver a mixture of phytochemicals to human colonic adenocarcinoma cell (CaCo-2) monolayers, *Br. J. Nutr. 91*, 757−764.
28. von Lintig, J., and Vogt, K. (2000) Filling the gap in vitamin A research. Molecular identification of an enzyme cleaving β-carotene to retinal, *J. Biol. Chem. 275*, 11915−11920.
29. von Lintig, J., Dreher, A., Kiefer, C., Wernet, M. F., and Vogt, K. (2001) Analysis of the blind *Drosophila* mutant *ninaB* identifies the gene encoding the key enzyme for vitamin A formation *in vivo*, *Proc. Natl. Acad. Sci. U.S.A. 98*, 1130−1135.
30. Rigotti, A., Miettinen, H. E., and Krieger, M. (2003) The role of the high-density lipoprotein receptor SR-BI in the lipid metabolism of endocrine and other tissues, *Endocr. Rev. 24*, 357−387.
31. Clayton, R. B. (1964) The Utilization of Sterols by Insects, *J. Lipid Res. 15*, 3−19.
32. Huber, A., Wolfrum, U., and Paulsen, R. (1994) Opsin maturation and targeting to rhabdomeral photoreceptor membranes requires the retinal chromophore, *Eur. J. Cell Biol. 63*, 219−229.
33. Vogt, K., and Kirschfeld, K. (1983) C40 Carotinoide in Fliegenaugen, *Verh. Dtsch. Zool. Ges. 76*, 330.
34. Giovannucci, D. R., and Stephenson, R. S. (1999) Identification and distribution of dietary precursors of the *Drosophila* visual pigment chromophore: Analysis of carotenoids in wild type and *ninaD* mutants by HPLC, *Vision Res. 39*, 219−229.
35. Eckhardt, E. R., Cai, L., Sun, B., Webb, N. R., and van der Westhuyzen, D. R. (2004) High density lipoprotein uptake by scavenger receptor SR-BII, *J. Biol. Chem. 279*, 14372−14381.
36. Eckhardt, E. R., Cai, L., Shetty, S., Zhao, Z., Szanto, A., Webb, N. R., and Van der Westhuyzen, D. R. (2006) High Density Lipoprotein Endocytosis by Scavenger Receptor SR-BII is Clathrin-dependent and Requires a Carboxyl-terminal Dileucine Motif, *J. Biol. Chem. 281*, 4348−4353.
37. Gronke, S., Beller, M., Fellert, S., Ramakrishnan, H., Jäckle, H., and Kühnlein, R. P. (2003) Control of fat storage by a *Drosophila* PAT domain protein, *Curr. Biol. 13*, 603−606.
38. Chapman, M. J. (1980) Animal lipoproteins: Chemistry, structure, and comparative aspects, *J. Lipid Res. 21*, 789−853.
39. Gu, G., Yang, J., Mitchell, K. A., and O'Tousa, J. E. (2004) *Drosophila* ninaB and *ninaD* act outside of retina to produce rhodopsin chromophore, *J. Biol. Chem. 279*, 18608−18613.
40. Combs, S. B., and Combs, G. F. (1985) Varietal Differences in the Vitamin E Content of Corn, *J. Agric. Food Chem. 33*, 815−817.
41. Parker, R. S., and McCormick, C. C. (2005) Selective accumulation of α-tocopherol in *Drosophila* is associated with cytochrome P450 tocopherol-ω-hydroxylase activity but not α-tocopherol transfer protein, *Biochem. Biophys. Res. Commun. 338*, 1537−1541.
42. Fluegel, M. L., Parker, T. J., and Pallanck, L. J. (2006) Mutations of a *Drosophila NPC1* gene confer sterol and ecdysone metabolic defects, *Genetics 172*, 185−196.
43. Rawson, R. B. (2003) The SREBP pathway: Insights from Insigs and insects, *Nat. Rev. Mol. Cell Biol. 4*, 631−640.
44. Chambon, P. (1996) A decade of molecular biology of retinoic acid receptors, *FASEB J. 10*, 940−954.

BI060701U